

## Supplementary Information

### **Singlet Fission Induced Giant Optical Limiting Responses of Pentacene Derivatives**

*Min Zhao<sup>a</sup>, Ke Liu<sup>a</sup>, You-Dan Zhang<sup>a</sup>, Qiang Wang<sup>a</sup>, Zhong-Guo Li<sup>b</sup>, Ying-Lin Song<sup>b</sup>,  
and Hao-Li Zhang<sup>a\*</sup>*

<sup>a</sup> State Key Laboratory of Applied Organic Chemistry, College of Chemistry and Chemical Engineering, Key Laboratory of Special Function Materials and Structure Design, Ministry of Education, Lanzhou University, Lanzhou 730000, P. R. China

<sup>b</sup> School of Physical Science and Technology, Soochow University, Suzhou 215006, P. R. China

<sup>c</sup> Department of Physics, Harbin Institute of Technology, Harbin 150001, P. R. China,

E-mail: [haoli.zhang@lzu.edu.cn](mailto:haoli.zhang@lzu.edu.cn)

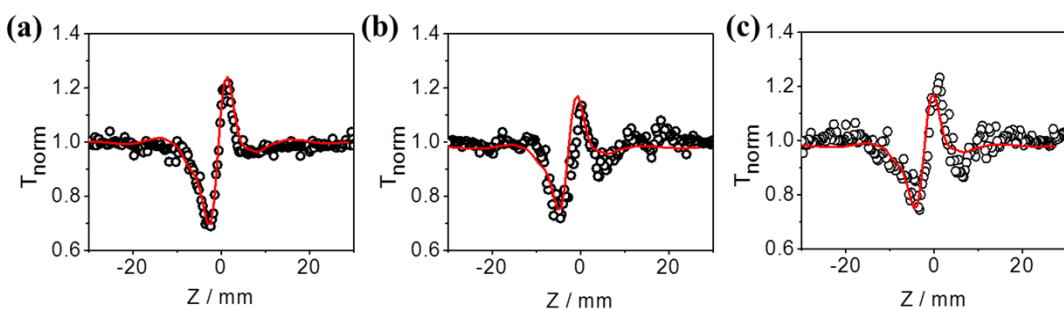


**Figure S1.** Closed aperture Z-scan data (symbols) and theoretically fitted curves (solid curves) of (a) TP, (b) 1NTP, (c) 4Cl1NTP obtained under the closed aperture conditions for 19 ps pulses at 532 nm. The solution spectra were collected in a 2.0 mm path length cell. The linear transmittance of all the samples given by the  $F_{out}/F_{in}$  ratio in the limit of zero fluence is 71%.

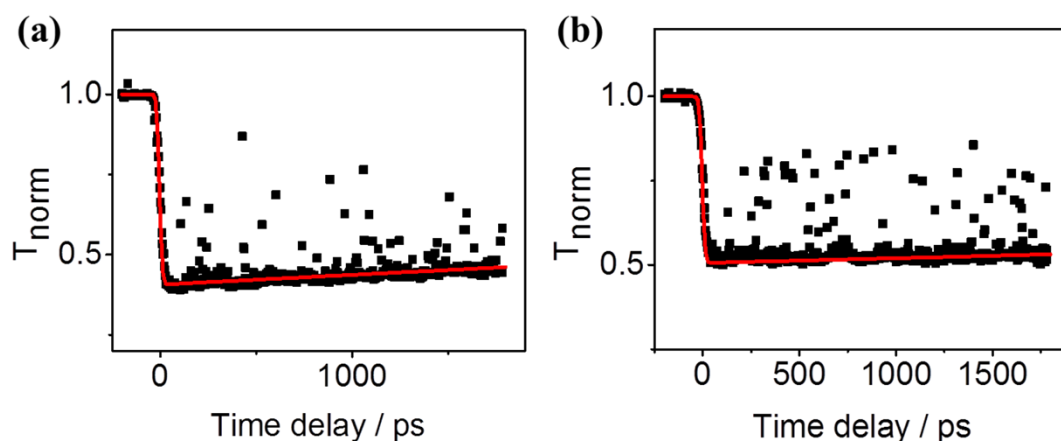


**Figure S2.** PO-pump-probe results for (a) 1NTP and (b) 4Cl1NTP (black dots: open aperture pump-probe results, red lines: theoretically fitted curves). The solution spectra were collected in a 2.0 mm path length cell. The linear transmittance of all the samples given by the  $F_{out}/F_{in}$  ratio in the limit of zero fluence is 0.57. Both pump and probe wavelengths were 532 nm.

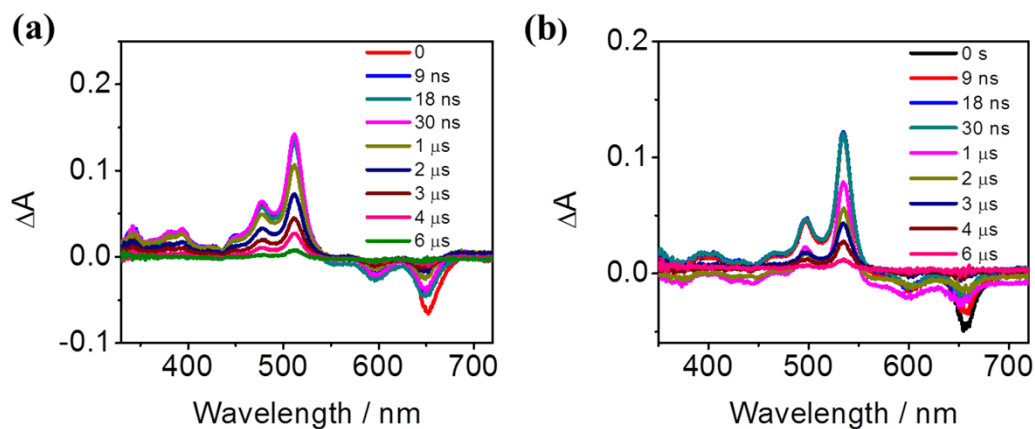


**Figure S3.** The transient absorption spectra of (a) 1NTP and (b) 4Cl1NTP in toluene on the time scale up to 6  $\mu$ s at a pump wavelength of 532 nm.

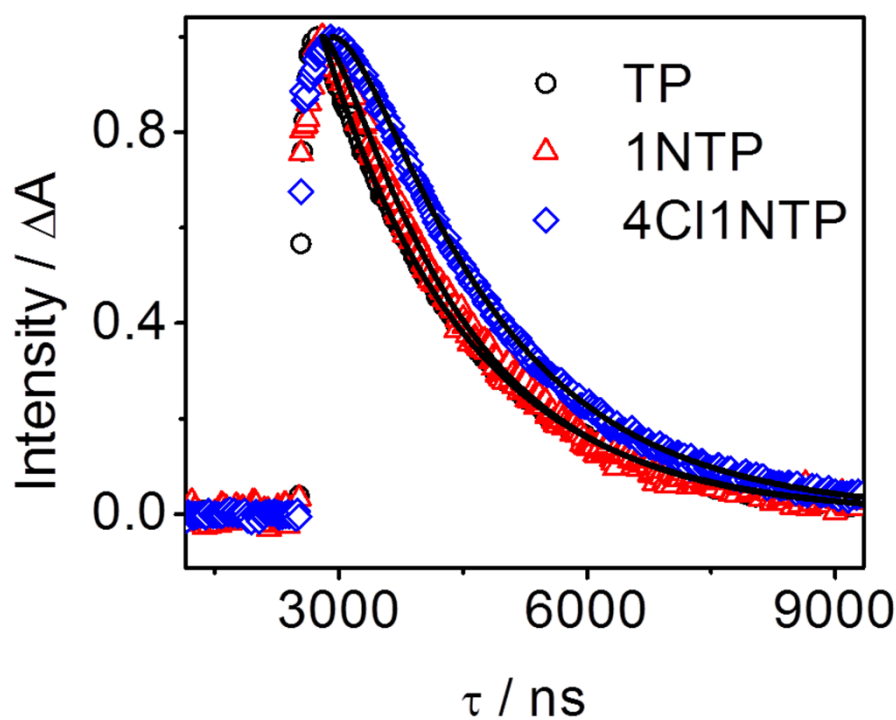


**Figure S4.** Decay profiles of excited state absorption of TP, 1NTP, 4Cl1NTP dissolved in toluene. The excitation wavelength was 532 nm and the decay curves were measured at 504 nm, 511 nm and 525 nm, respectively. A significant long lifetime of  $\sim 1.7 \mu$ s can be extracted for all of the samples.

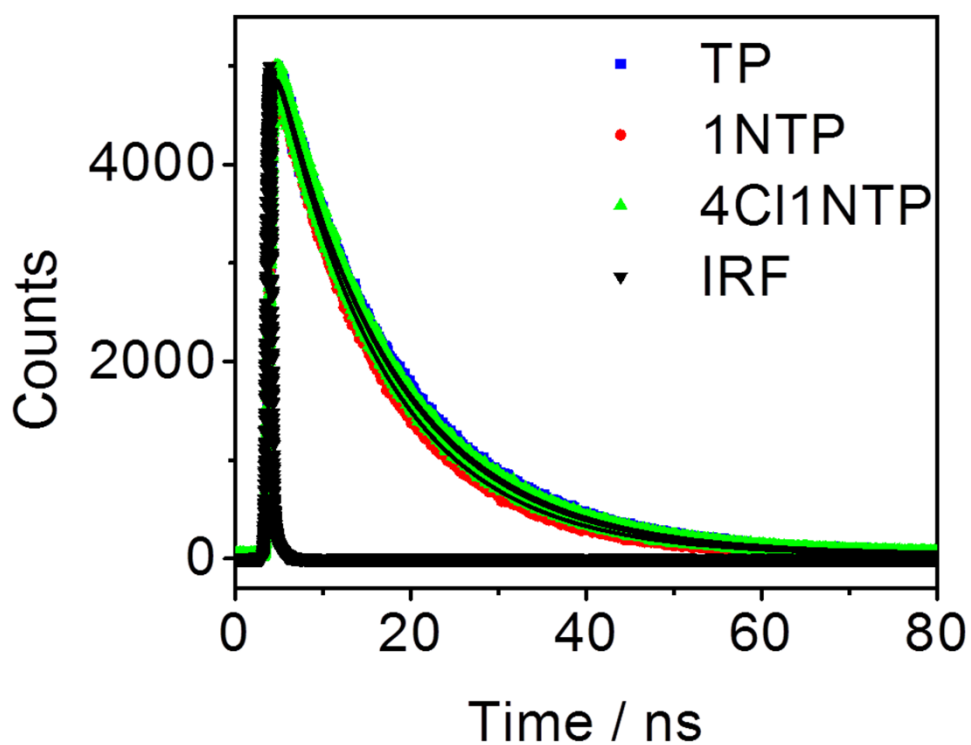


**Figure S5.** Photoluminescence decay profiles of TP, 1NTP, 4Cl1NTP dissolved in toluene. The excitation wavelength was 464 nm and the decay curves were measured at 657 nm. Monoexponential fitting of the data gave lifetime of  $14.2 \pm 0.3$  ns,  $12.5 \pm 0.2$  ns and  $13.3 \pm 0.3$  ns for TP, 1NTP and 4Cl1NTP respectively.

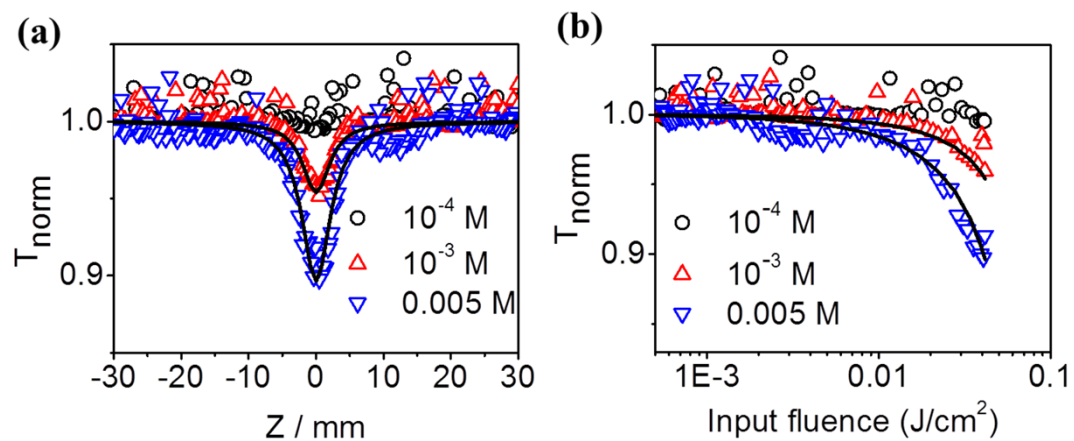


**Figure S6.** (a) Open aperture Z-scan data and theoretically fitted curves, and (b) corresponding plot of transmittance versus input fluence and theoretically fitted curves (solid curves) using 19 ps pulses at 532 nm for  $C_{60}$  at different concentrations.

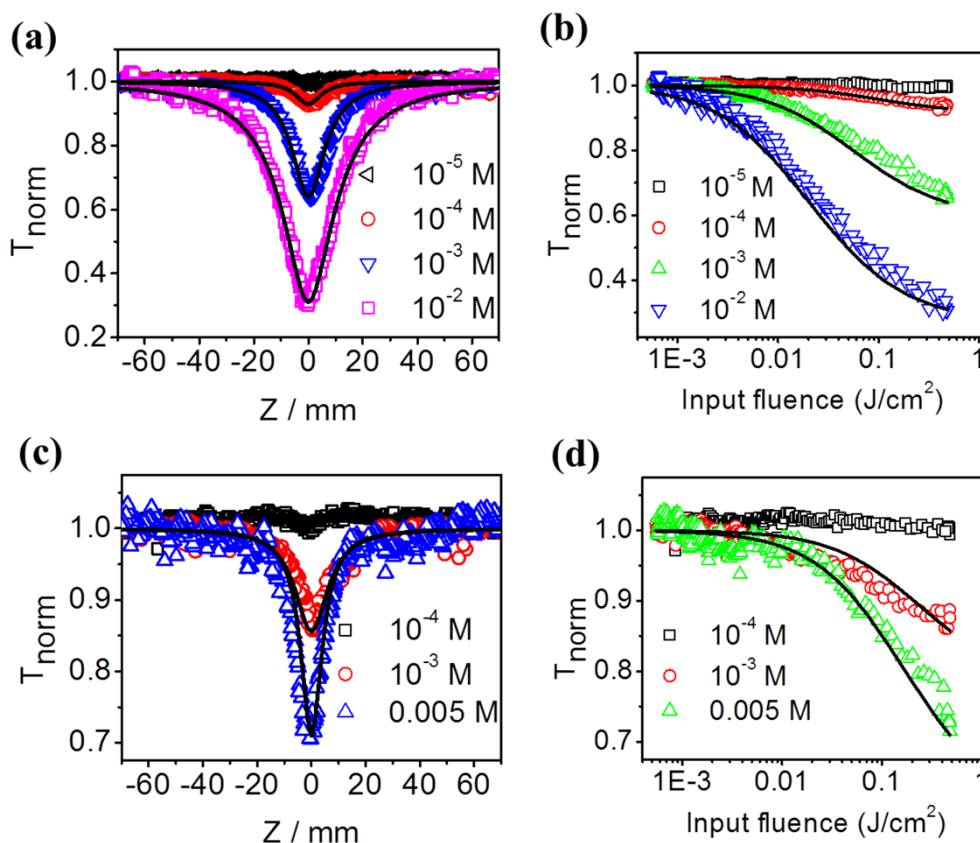


**Figure S7.** (a) Open aperture Z-scan data and theoretically fitted curves, and (b) corresponding plot of transmittance versus input fluence and theoretically fitted curves (solid curves) using 4 ns pulses at 532 nm for TP at different concentrations. (c) Open aperture Z-scan data and theoretically fitted curves, and (d) corresponding plot of transmittance versus input fluence and theoretically fitted curves (solid curves) using 4 ns pulses at 532 nm for C<sub>60</sub> at different concentrations.

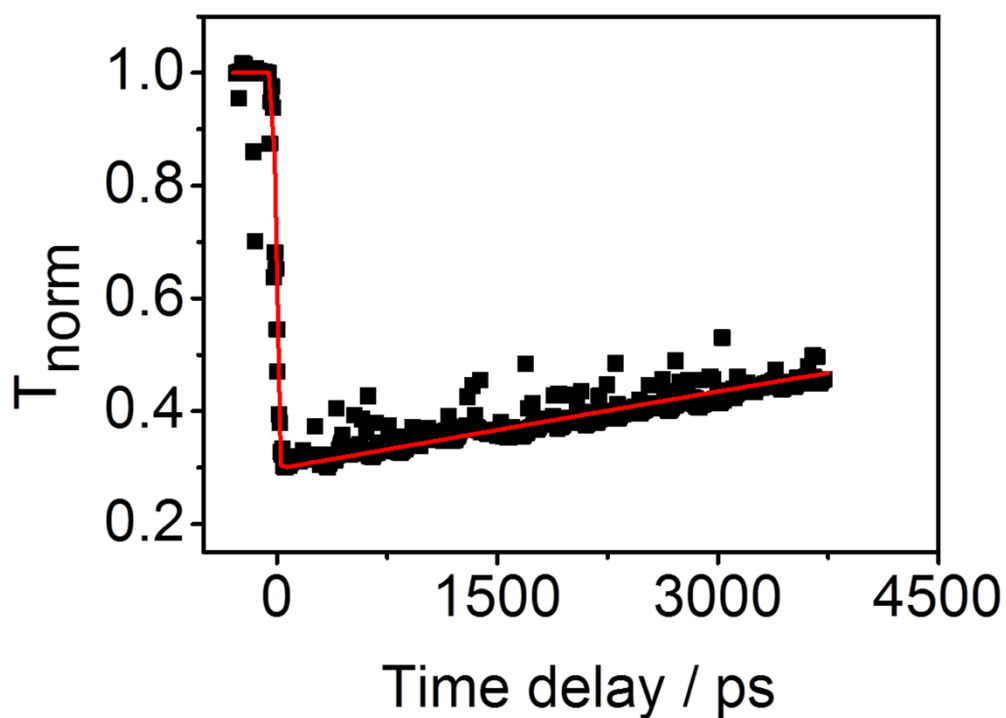


**Figure S8.** PO-pump-probe results for concentrated TP solution (0.01 M) (black dots: open aperture pump-probe results, red lines: theoretically fitted curves). The solution spectra were collected in a 0.2 mm path length cell. The linear transmittance of all the samples given by the  $F_{\text{out}}/F_{\text{in}}$  ratio in the limit of zero fluence is 0.21. Both pump and probe wavelengths were 532 nm.

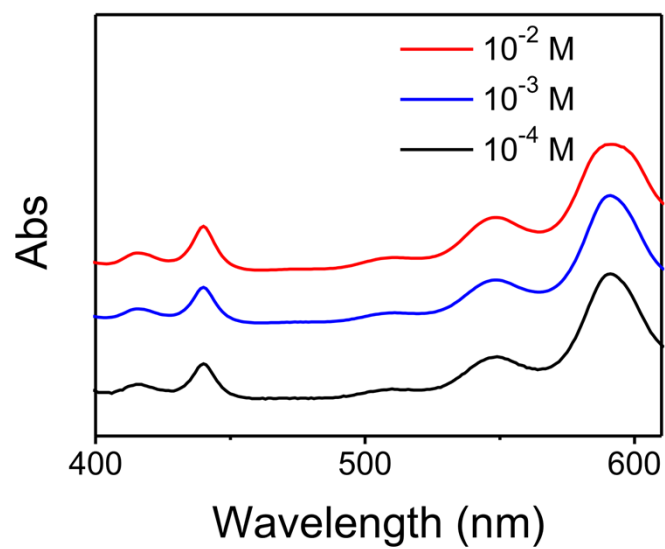


**Figure S9.** UV-vis spectra of TP at different concentrations in toluene.

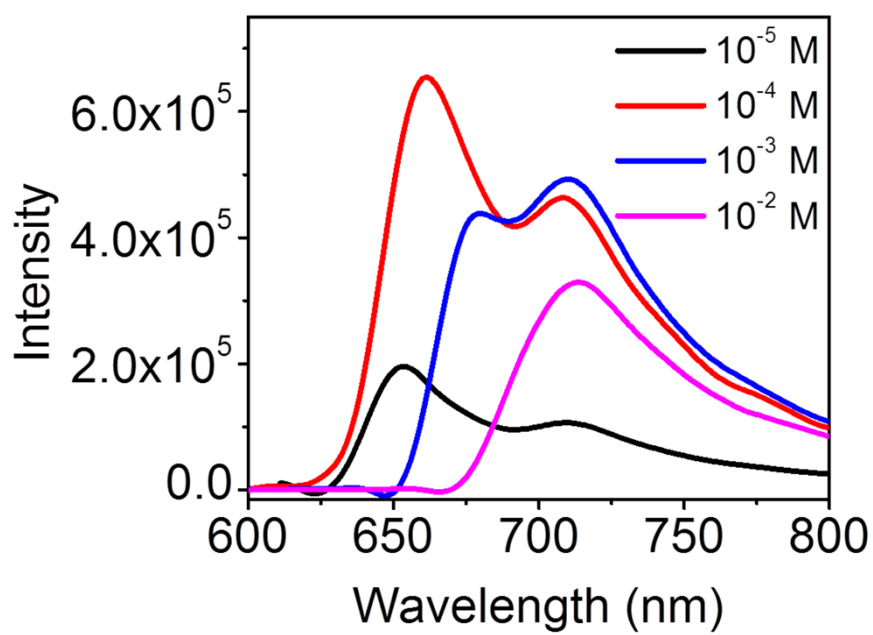


**Figure S10.** Fluorescence spectra of TP at different concentrations in toluene



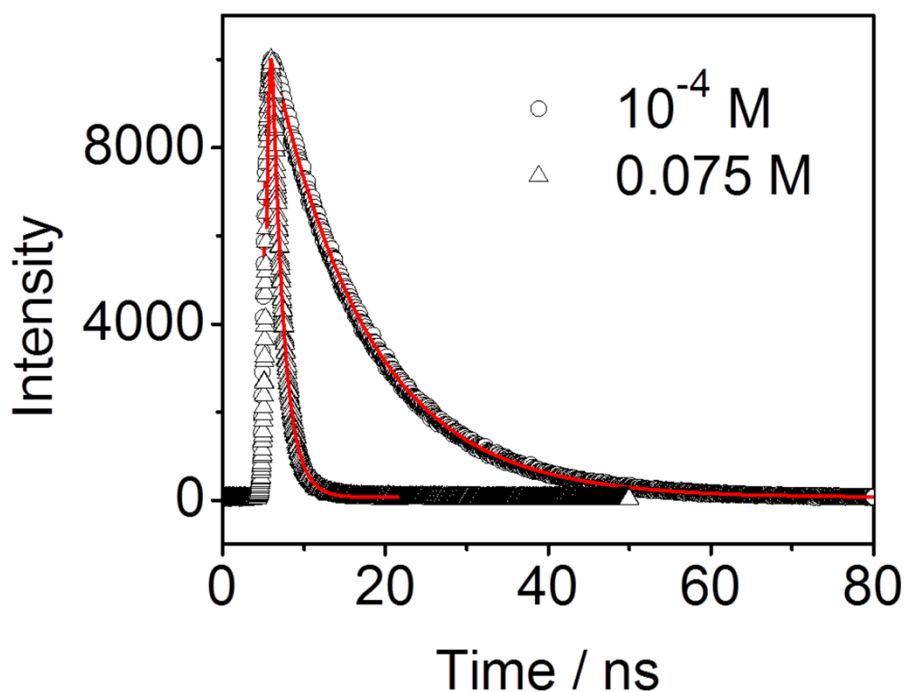


**Figure S11.** Photoluminescence decay profiles of TP dissolved in toluene at different concentrations. The red lines are theoretically fitted curves.

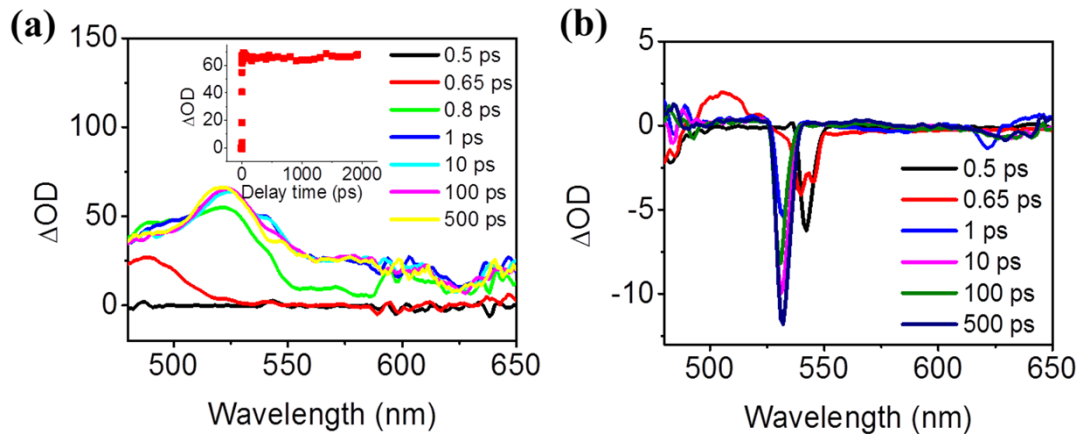


**Figure S12.** Transient absorption spectra of TP dissolved in toluene at different concentrations (a) 0.01M and (b) 0.0001 M at a pump wavelength of 532 nm. The inset in Figure (a) reflects the decay profiles at 520 nm.

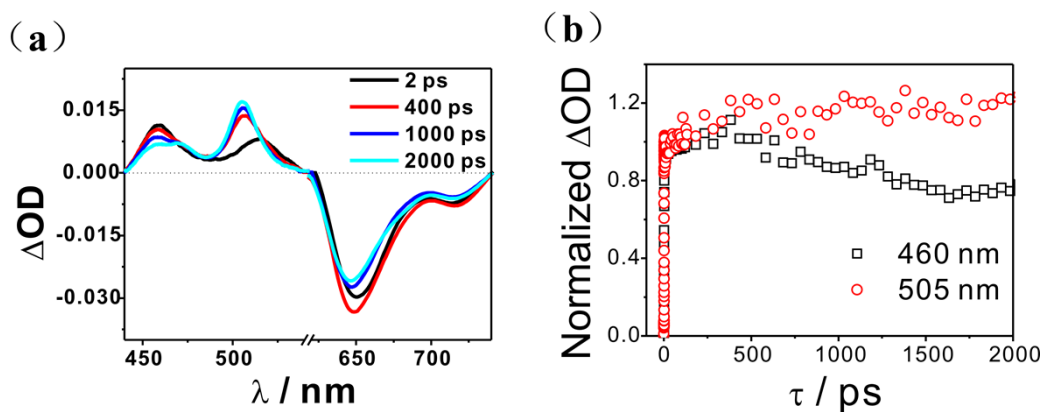


**Figure S13.** (a) Transient absorption spectra and (b) kinetic traces at indicated wavelengths of TP dissolved in toluene at the concentration of 0.01 M. The ground-state bleach at 650 nm has both a delayed increase and a decay, which constitutes direct evidence for singlet fission.

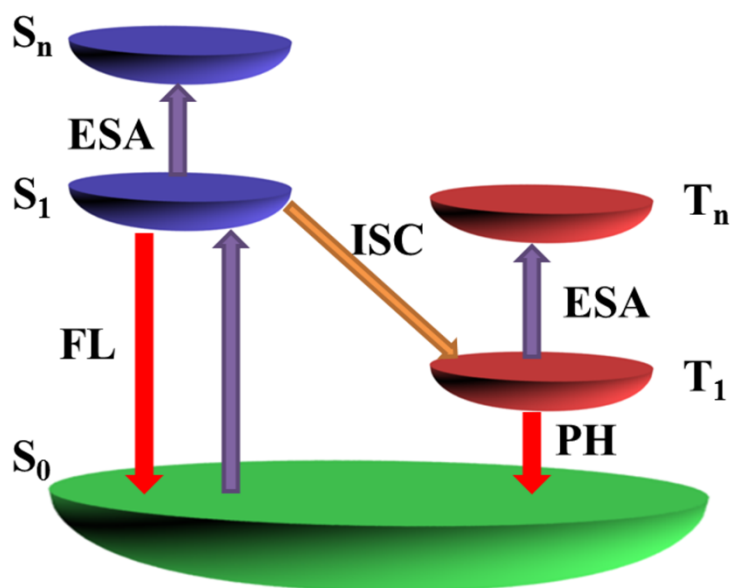


**Figure S14.** An energy level model demonstrating the pentacene derivatives respond on both fast and slow timescales in dilute solution. (FL: fluorescence; PH: phosphorescence; ESA: excited state absorption; ISC: intersystem crossing )

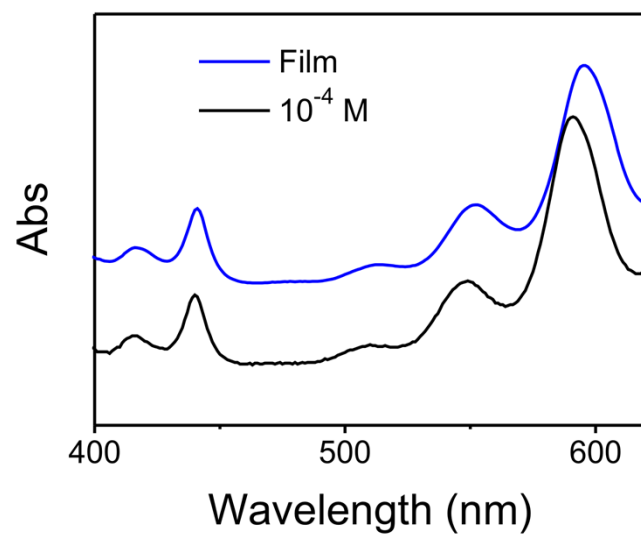


**Figure S15.** UV-vis spectra of TP in toluene (black line) at the concentration of  $10^{-4}$  M and in polystyrene film (blue line).

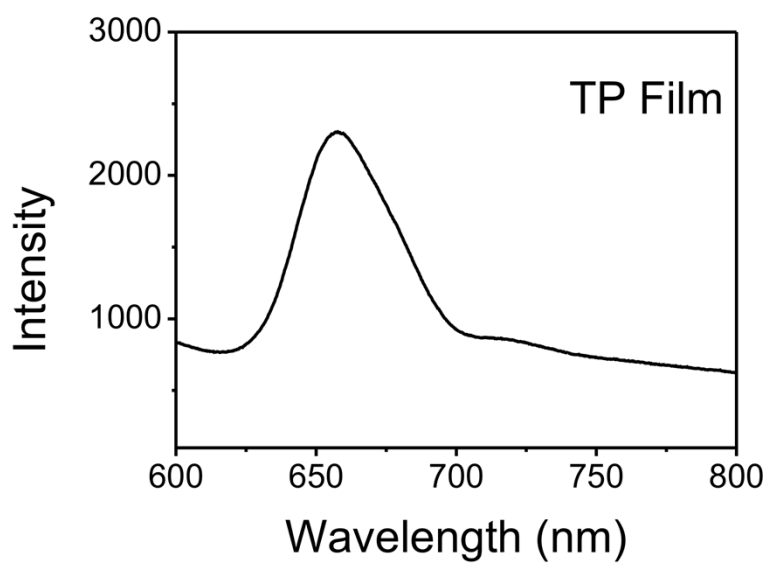


**Figure S16.** Fluorescence spectra of TP in the polystyrene film.

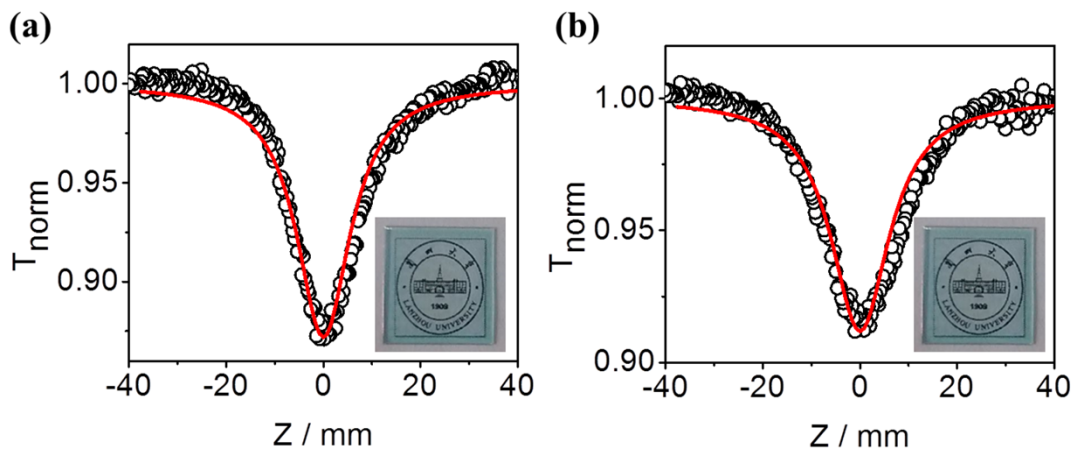


**Figure S17.** Open aperture Z-scan data for a neat film of (a) 1NTP, (b) 4Cl1NTP in polystyrene irradiated by 4 ns pulses at 532 nm. The solid curve is numerical fit for data. The linear transmittance of the sample given by the  $F_{\text{out}}/F_{\text{in}}$  ratio in the limit of zero fluence is 0.85. Inset: photograph of film cast on fused silica.

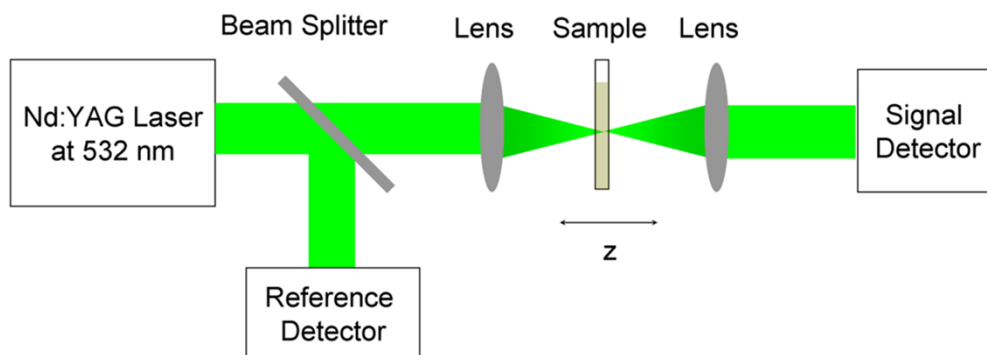


**Figure S18.** Schematic representation of the Z-scan experimental arrangement.

**Z-scan measurement<sup>1-3</sup>:** For a nanosecond Z-scan measurement, 5 ns (FWHM), 532 nm laser pulses with a repetition rate of 10 Hz from a frequency-double Q-switched Nd:YAG laser (Continuum, Model Surelite SL-I-10) was used as the light source. The spatial and temporal profiles of the laser pulses presented an approximately Gaussian distribution. The output laser beam with nearly Gaussian distribution was split into

two beams: a reference beam to monitor energy fluctuations and a strong beam in a tightly focused geometry. The quartz cell was placed on a translation stage controlled by a computer that moved along the Z-axis with respect to the focal point of a 410 mm convex lens. The beam waist radius equal to 20  $\mu\text{m}$  with a Rayleigh length  $Z_R$  of 2362  $\mu\text{m}$ . This Rayleigh length was much larger than the thickness of the sample. Two corresponding pyroelectric detectors (Laser Probe, RJ-735; with RJ7620 dual channel power meter) were used to measure changes in laser transmission. Under the open-aperture configuration, the aperture placed before the detector was kept open and the nonlinear absorption of the samples was measured. The other part of laser beam was simultaneously measured by another detector with a partially closed aperture set in front of it, which is the close-aperture configuration. The intensity change detected herein contained both nonlinear absorption and nonlinear refraction. The Z-scan curve, which is the normalized transmittance as a function of the sample position, was measured with and without an aperture in the far field. Herein, we used normalized transmittance, which equals to the ratio of nonlinear and linear transmittance, as a standard to study the NLO properties pentacene derivatives. The samples were placed in quartz cells with thickness of 2 mm, mounted on a translation stage that was controlled by a computer to move along the Z axis with respect to the focal point. In this measurement, normalized transmittance of 1.0 indicates that the material exhibits no NLO behavior. When the sample exhibits saturable absorption, normalized transmittance above 1.0 will be observed. In contrast, the normalized transmittance below 1.0 indicates that the sample exhibits reverse saturable absorption.

For optical limiters, the measured curves would exhibit valleys at the focus and the deeper the valley, the stronger the optical limiting performance of the material.

For a picosecond Z-scan measurement, the laser was simply replaced by a Q-switched and mode locked Nd:YAG laser (EKSPLA PL2143B) with pulse width of 19 ps (FWHM) as the light source while all of the other parts remain unchanged.

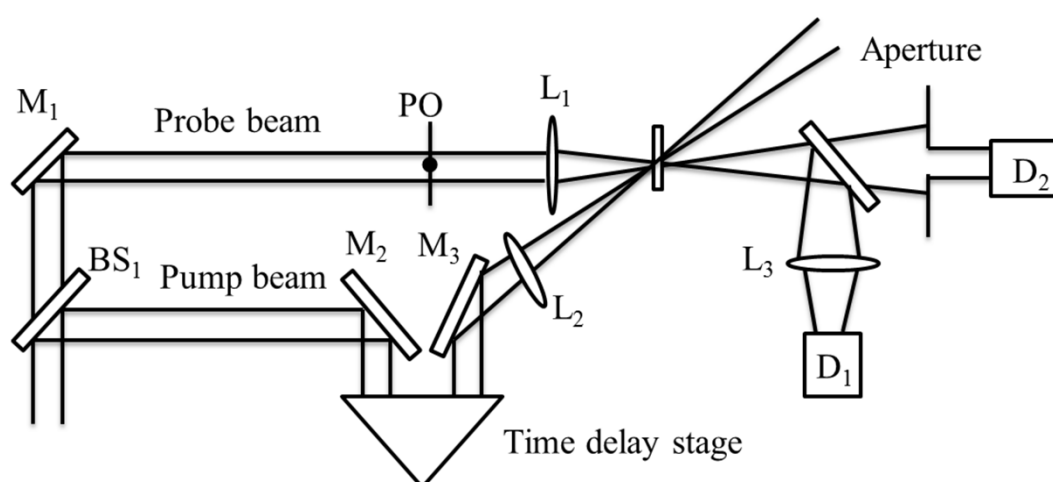


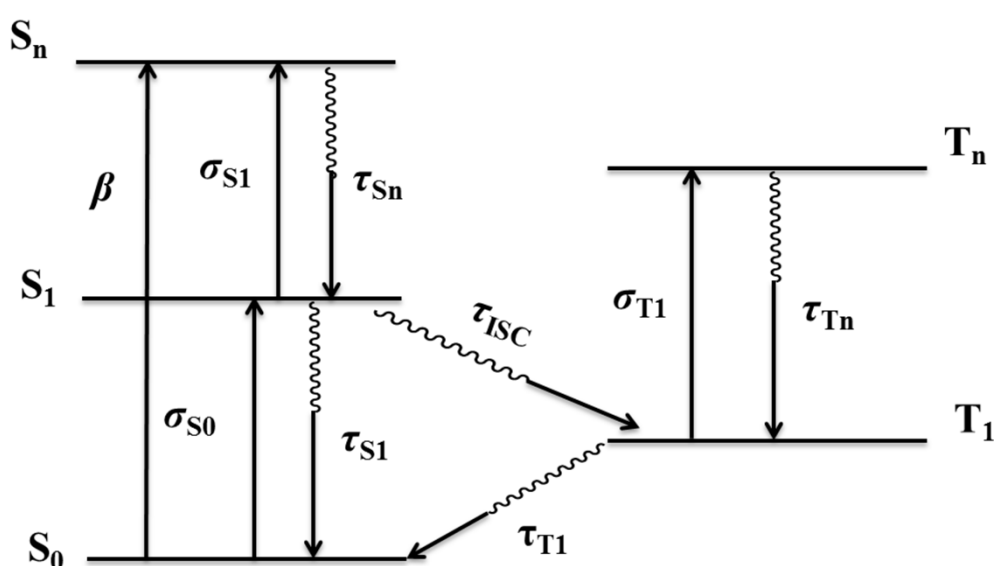
**Figure S19.** Schematic representation of the PO-pump-probe experimental arrangement.

**PO-pump-probe measurement:** The PO-pump-probe setup is a new time-resolved pump-probe system with phase object, based on the PO Z-scan technique and the standard pump-probe system<sup>4-6</sup>. This setup is capable of simultaneously investigating the dynamics of nonlinear absorption and refraction. Meanwhile, in principle both degenerate and nondegenerate pump and probe beams in any polarization states can be employed in this system. Herein we adopt the degenerate scheme with the pump

and probe wavelength both at 532 nm. All the nonlinear optical measurements were carried out at room temperature. The experimental setup for the PO-pump probe experiment is shown in Fig S15. The laser source was a Q-switched and mode locked Nd:YAG laser (EKSPLA PL2143B) with pulse width of 19 ps (FWHM). The spatial profile of the laser beam was nearly Gaussian distribution. The laser beam was split into two parts with a 3:1 intensity ratio by the beam splitter BS<sub>1</sub>. The strong pump beam was time-delayed using a motorized computer-controlled delay line (physik instrumente, M531). The polarization direction of pump beam was adjusted to be perpendicular to that of probe beam by a half-wave plate (HWP). The circular radius of the dielectric is  $L_p = 0.5$  mm, and it gives a phase retardation of  $\phi_L = 0.45 \pi$  for the 532 nm optical wave. The pump and probe beams were focused to a common spot on the quartz cuvette (path length 2 mm) using two identical convex lens with a focal length of 41 cm. After the sample, the probe beam propagated to the far field where a circular aperture was placed. Because of its small diameter, only the probe beams which passing through the PO's central dielectric could transmit and detected by detector D2. The distance between the aperture and the sample was 0.8 m, and the radius of the aperture was 0.75 mm. The energy were recorded by two silicon detector (Laser Probe, Rjp-765a) simultaneously, and measured by a dual-channel power meter (Rj-7620, Laser Precision Corp.) which transferred the digitized signals to a computer via GPIB interface.

**PO-pump-probe and Z-scan data fitting routine:** Our fitting method is simultaneous fits to the PO-pump-probe and Z-scan experimental data to extract

parameters such as absorption cross sections and excited state lifetimes associated with different energy levels, by means of solving a set of differential equations numerically, including rate equations based on a classic five-level model for organic compounds and laser beam propagating equations<sup>5, 6</sup>. Based on the following classic five-level model for organic compounds, the rate equations for these various processes can be described as:



**Supplementary Figure S20.** A classic five-level model for organic compounds

$$\frac{dN_{S0}}{dt} = -\frac{\sigma_{S0}I_e N_{S0}}{\hbar \omega} - \frac{\beta I_e^2}{2\hbar \omega} + \frac{N_{S1}}{\tau_{S1}} + \frac{N_{T1}}{\tau_{T1}} \quad (1)$$

$$\frac{dN_{S1}}{dt} = -\frac{\sigma_{S1}I_e N_{S1}}{\hbar \omega} + \frac{\sigma_{S0}I_e N_{S0}}{\hbar \omega} - \frac{N_{S1}}{\tau_{S1}} - \frac{N_{S1}}{\tau_{ISC}} + \frac{N_{Sn}}{\tau_{Sn}} \quad (2)$$

$$\frac{dN_{Sn}}{dt} = \frac{\sigma_{S1}I_e N_{S1}}{\hbar \omega} + \frac{\beta I_e^2}{2\hbar \omega} - \frac{N_{Sn}}{\tau_{Sn}} \quad (3)$$

$$\frac{dN_{T1}}{dt} = -\frac{\sigma_{T1}I_e N_{T1}}{\hbar \omega} - \frac{N_{T1}}{\tau_{T1}} + \frac{N_{S1}}{\tau_{ISC}} + \frac{N_{Tn}}{\tau_{Tn}} \quad (4)$$



$$\frac{dN_{Tn}}{dt} = -\frac{\sigma_{T1} I_e N_{T1}}{\hbar \omega} - \frac{N_{Tn}}{\tau_{Tn}} \quad (5)$$

where  $N_i$  is the population density for state  $i$ , with a corresponding absorption cross section  $\sigma_i$ ;  $S_n$  is the  $n$  th singlet state;  $T_n$  is the  $n$  th triplet state;  $\tau_i$  is the lifetime for state  $i$ .  $\tau_{ISC}$  is the intersystem crossing time. In the case of the occurrence singlet fission,  $\tau_{ISC}$  is replaced by the singlet fission time constant.  $\hbar$  is the Planck constant;  $\omega$  is the optical frequency, and  $I_e$  is the pump intensity.

In combination with the following laser beam propagating equations:

$$\frac{dI_p}{dz} = -(\sigma_{S0} N_{S0} + \sigma_{S1} N_{S1} + \sigma_{T1} N_{T1} + 2\beta I_e) I_p \quad (6)$$

$$\frac{d\varphi_p}{dz} = k(\Delta\eta_{S1} N_{S1} + \Delta\eta_{T1} N_{T1} + 2n_2 I_e) \quad (7)$$

$$\frac{dI_e}{dz} = -(\sigma_{S0} N_{S0} + \sigma_{S1} N_{S1} + \sigma_{T1} N_{T1} + \beta I_e) I_e \quad (8)$$

where  $\beta$  is the two-photon absorption coefficient;  $n_2$  is the Kerr refraction;  $I_p$  is probe intensity;  $\varphi_p$  is the probe phase;  $\Delta\eta_i$  is the change of refraction index per unit density of state  $i$ , and  $z$  is the propagation length within the sample. Then parameters such as absorption cross sections and excited state lifetimes associated with different energy levels can be extracted by solving the above set of differential equations numerically.

## References

- (1) Sheikbahae, M.; Said, A. A.; Wei, T. H.; Hagan, D. J.; Vanstryland, E. W., *IEEE J. Quantum Electron.* **1990**, *26*, 760.

- (2) Wang, T. M.; Gao, B.; Wang, Q.; Zhao, M.; Kang, K. B.; Xu, Z. G.; Zhang, H. L., *Chem. Asian. J.* **2013**, 8, 912.
- (3) Li, Z.-G.; Lu, Y.-T.; Yang, J.-Y.; Nie, Z.-Q.; Shui, M.; Jin, X.; Ge, J.-F.; Song, Y.-L., *Mater. Chem. Phys.* **2013**, 139, 975.
- (4) Yang, J.; Song, Y., *Opt. Lett.* **2009**, 34, 157.
- (5) Shi, G.; He, C.; Li, Y.; Zou, R.; Zhang, X.; Wang, Y.; Yang, K.; Song, Y.; Wang, C. H., *J. Opt. Soc. Am. B-Optical Physics* **2009**, 26, 754.
- (6) Yang, J.; Song, Y.; Wang, Y.; Li, C.; Jin, X.; Shui, M., *Opt. Express* **2009**, 17, 7110.